Journal of Imaging Science and Technology® 57(5): 050506-1–050506-7, 2013.

Inkjet Printing and Sintering of Nano-Copper Ink

Sooman Lim, Margaret Joyce, Paul D. Fleming▲, and Ahmed Tausif Aijazi
Department of Chemical and Paper Engineering, Western Michigan University, 4601 Campus Dr. # A-217, Kalamazoo, MI 49008
E-mail: Sooman.lim@gmail.com

Massood Atashbar
Department of Electrical and Computer Engineering, Western Michigan University, 4601 Campus Dr. # A-217, Kalamazoo, MI 49008

Abstract. *An alternative low-cost replacement for silver and gold conductive inks is of great interest to the printed electronics industry. Nanoparticle copper inks and silver-coated nano-copper inks are some of the alternative materials being tested for use, especially in applications where low-temperature flexible substrates are favored. Although the inkjettability of nano-copper ink and the influence on print quality has been reported, information regarding the relationship between the ink film thickness and the energy required for sintering by intensive pulse light is not yet understood. In this study, an inkjettable nano-copper ink was printed on PET (polyethyleneterephthalate) and glass, and the samples were sintered using bursts of high-intensity pulsed light. The amount of energy applied determined the degree of sintering among particles. The greater the number of sintered nanoparticles, the higher is the conductivity of the printed traces. A comparison of energy levels required for sintering on glass and PET in relationship to the ink film thickness is reported, and the thermal contribution of the substrate to the processing energy requirements of this ink is revealed. © 2013 Society for Imaging Science and Technology.*
[DOI: 10.2352/J.ImagingSci.Technol.2013.57.5.050506]

INTRODUCTION

Inkjet printing is an attractive printing technology for the deposition of functional inks, due to its advantages of low cost and the ability to print fine lines and thin layers, and due to the wide range of available materials available for printing by this method. Although inkjet printing of silver and gold is already being practiced, their high costs have limited their use, especially for low-cost flexible electronic applications. As a result, low-cost alternative materials are of interest. The use of conductive organic polymers, organo-metallic compounds, metal precursors, and metal-based nanoinks has all been reported, with different print methods being employed for their deposition. Although conductive polymers meet the requirements in terms of being used in soluble deposition printing, their low conductivity and instability to the air are significant shortcomings.[1] Metal precursor and organo-metallic compounds require a heat treatment for reduction, which leaves residual organic matter in the fabricated film that may adversely affect the product performance.[2] For metal-based nanoinks, the requirement for low-temperature in situ sintering of the inks is an issue.[3] Kim and Moon[4] sintered Ag nanoink at 200°C for 30 min in a thermal oven, and found that the conductivity was changed based on the sintering temperature and size of the nano-Ag particles applied. Ko et al.[5] used a localized sintering technique to sinter nano-Au particles on polyimide films, but found that the sintering technology used was not useful over a large area.

To address the high throughput needs for roll-to-roll (R2R) processing and the desire for a low-cost alternative to Ag and Au inks, the use of intensive pulsed light (IPL) generated from a xenon lamp source, to sinter nano-copper ink particles under ambient conditions, was examined.[6] IPL delivers a quick burst of intense near-UV energy to the printed surface. The intensity of energy, the duration of the pulse, and the distance from the printed surface can all be varied to alter the amount of energy applied. Due to the short time interval (milliseconds) of the light pulses, the nanoparticles can be sintered without damage to the underlying substrate layer. This makes it appropriate for use with PET film and paper for flexible printed electronic applications. For copper-based inks, conductivity is achieved through either the conversion of CuO nanoparticles to Cu, or vaporization of a protective coating layer applied to the Cu nanoparticles to prevent oxidation prior to sintering. Although the mechanism for conversion of these inks from the non-conductive to the conductive state is understood, until now, the relationship between the ink film thickness and the amount of irradiated energy required for sintering has not yet been examined.

In this work, the inkjet printability, print quality, and electrical properties of a new commercially available nanoparticle copper ink were studied on PET and glass before and after sintering. The inks were printed using a Dimatix DMP-2800 inkjet printer. Sintering was performed using a Xenon Sinteron 2000 unit. The amount of energy applied was controlled by varying the applied voltage, the duration of the pulse, and the number of pulses. The extent of particle sintering was examined under high magnification with a scanning electron microscope (SEM).

EXPERIMENT

A commercial nano-copper ink, CI-002 (Intrinsiq Materials, UK) containing 25 nm diameter[7] particles (10 wt%) and with density 1.2 g/cm^3 was used to print multiple 1 cm × 0.5 cm

▲ IS&T Member.

Received Feb. 12, 2013; accepted for publication Aug. 22, 2013; published online Sep. 1, 2013. Associate Editor: Hiroyuki Kawamoto.
1062-3701/2013/57(5)/050506/7/$20.00

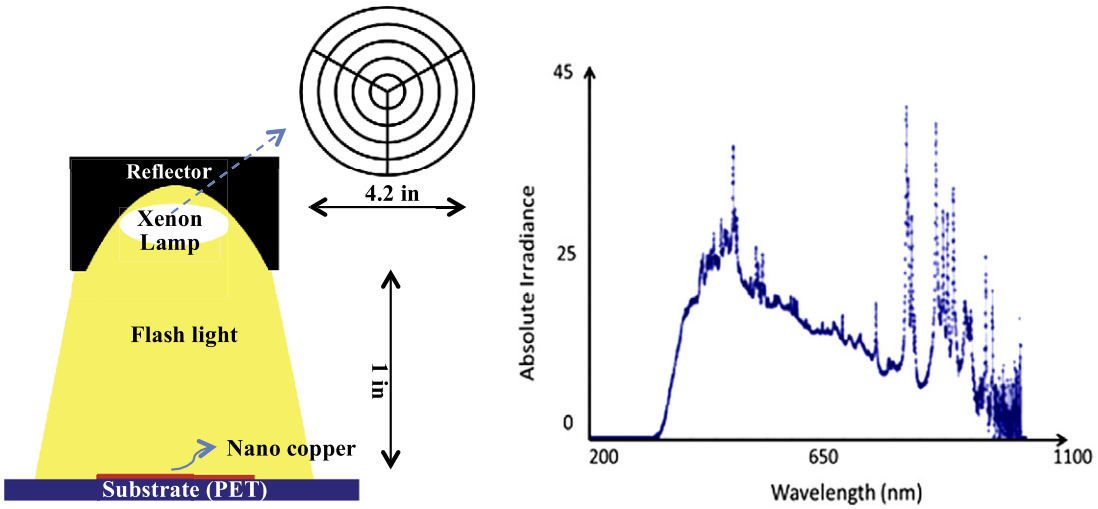

Figure 1. Schematic of the intensive pulsed light sintering system (a), spectral distribution of the xenon lamp with the 3600 V and 15 Hz setup (b).

rectangular samples. Since the ink was encapsulated with an organic coating (patented process[8]), the ink was uniformly dispersed in a mixture of ethane-1,2-diol (ethylene glycol) and n-butanol and stable under ambient conditions. The samples were printed at different drop spacing intervals (10, 20, and 30 μm) using a Dimatix DMP-2800 inkjet printer (Fujifilm, CA). Prior to printing, the inks were characterized by measuring the surface tension and rheological properties with an FTA 200 (First Ten Angstroms, Inc., VA) dynamic contact angle measuring device and an RA 2000 dynamic stress rheometer (TA Instruments, DE), respectively. The surface energy of the ink was estimated at room temperature using the Owens–Wendt model[9] with high-purity water and methylene iodide as test fluids. Since the jetting performance of an inkjet ink strongly depends on its dimensionless Z-number, this value was calculated from viscosity, surface tension, density, and drop diameter (nozzle orifice) measurements.[10,11] Viscosity measurements were performed at a fixed shear rate of 10 s^{-1}, which was determined to be in the second linear plateau region of the steady-flow curve obtained for this ink (see Figure 4). Surface tension was measured by the pendant drop method. Prior to printing, the ink was placed into an ultrasonic bath for one hour to ensure homogeneity and degassing of the ink. The ink was then injected into a 10 pL cartridge and loaded into the DMP, where it was allowed to equilibrate for 30 min. The waveform and temperature range of the cartridge (from 28 to 70°C) were then adjusted by observing the ink-jetting behavior and the drop formation of the ink through a drop watcher camera until satisfactory jetting was achieved[10] (no satellite drops or puddling at the nozzle). Two substrates were printed: a 127 μm PET film Melinex ST505 (dupont teijin films, delaware) and a 614 μm glass film (alkaline earth boro-aluminosilicate type). After printing, the samples were immediately sintered (sinteron 2000, xenon Corporation, MA). The least amount of energy required to obtain the lowest electrical resistance, without damage to the ink film or substrate, was determined by inspecting each sample after sintering and measuring its electrical resistance using a four-point probe. The IPL system consisted of a 15 cm diameter xenon spiral Type B lamp,[12] power supply, capacitors, lamp flash control panel, and air-cooling system, as illustrated in Figure 1(a). The spiral lamp irradiated over a wide wavelength spectrum in the range from 330 to 1050 nm, as shown in Fig. 1(b).

Using Eq. (1), the electrical energy per pulse was calculated:

$$\frac{\{C \times (V)^2\}}{2} = Electrical\ Energy/pulse, \qquad (1)$$

where C and V refer to capacitance and voltage applied to the system, respectively. The pulse energy was varied from 5175 to 10 909 J, while the capacitance and pulse duration were fixed at 82 F and 500 μs, respectively. During printing of the samples, it was observed that the ink did not wet the PET film well, resulting in incomplete coverage and poor uniformity of the ink film. To improve the wetting, the film was treated with UV/ozone (Jelight Inc., CA) for up to 275 s. The UV/ozone treatment raised the surface energy of the film, promoting better wetting, which improved the quality of the printed ink film.

As a first step after printing, each sample received a single pulse flash, after which the sheet resistance was measured using a four-point probe-sensing mode (multimeter model 2400, Keithley, OH). If the sample was non-conductive, the IPL treatment procedure was repeated. Based on the results, changes were made to increase the pulse energy by adjusting the lamp voltage in order to minimize the number of pulses required. Once the number of pulses and voltage required to obtain the lowest resistance for each sample was determined, on average, three samples for each substrate were treated and three resistance measurements per sample were taken. The quality of the printed pattern was analyzed using an ImageXpert, Inc. image analyzer.

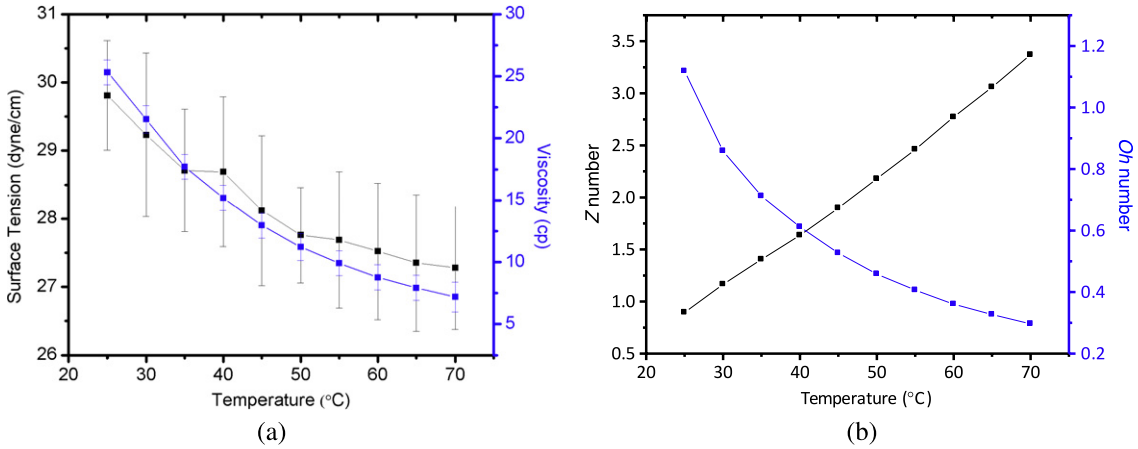

Figure 2. Change in surface tension and viscosity (a), Z-number and Ohnesorge number (b).

Next, the surface of sintered samples was examined under a scanning electron microscope and a Wyko white light interferometry microscope. Adhesion tests were performed using a Friction/Peel Tester Model 225 (Thwing Albert Instrument Company, PA), equipped with a diamond tip attached to a sled containing a 1 kg weight, which was dragged across the surface of the samples at 0.1 cm/s.

RESULT AND DISCUSSION

In order to predict the inkjettability of the nano-copper ink on the Dimatix DOD inkjet printer, the Z-number was calculated according to Eq. (2). This number is the reciprocal of the Ohnesorge number[13]

$$Z = \frac{Re}{\sqrt{We}} = (d\rho\sigma)^{\frac{1}{2}}\frac{1}{\eta} = Oh^{-1}(Ohnesorge\ number), \quad (2)$$

where η, ρ, and σ are the viscosity, density, and surface tension of the liquid, respectively, and d is the diameter of the nozzle aperture (21.5 μm). The Z-number is important, because it predicts the drop formation quality through an inkjet nozzle.[10,11,13]

As a first step to calculate the Z-number, the change in surface tension and viscosity of the ink with temperature was measured. As shown in Figure 2(a), the temperature of the ink was increased from 25°C (room temperature) to 70°C (maximum attainable cartridge temperature adjustment). The properties of the ink were measured at elevated temperature because it was determined that elevated temperatures were needed for good jetting. The change in Z-number and Ohnesorge number with change in surface tension and viscosity is shown in Fig. 2(a), (b). As a consequence of heating, both the surface tension and viscosity of the ink decreased, which consequently resulted in the lowering of the Z-number. According to Reis et al.,[11] for best jetting, the Z-number should fall between 1 and 10. As shown in Fig. 2(b), the Z-number does not meet this criterion at 25°C, but this criterion is met at any temperature above 27°C. However, in practice, it was found that a minimum cartridge temperature of 34°C at an applied voltage of 40 V was needed to jet the ink.[10] Under these conditions, a drop speed of 2 m/s is accomplished with good jetting characteristics.

Although the 34°C temperature was higher than what was expected to be needed for good jetting, at this temperature, the Z-number (1.35) does fall within the theoretical Z-number range for good jetting. In general, for good jetting the kinetic energy applied to the drop needs to be higher than the surface tension energy of the liquid and the viscous dissipation of the liquid for drop ejection to occur. This means that a high surface tension and viscosity ink will require more kinetic energy to expel it from the cartridge.[13] Based on this reasoning, the ink did not jet well at room temperature due to its viscosity and surface tension being higher than the kinetic energy that could be generated by the waveform. Practically, the measured viscosity of 28.3 cp at room temperature was much higher than the 1–12 cp range recommended by Dimatix. Increasing the cartridge temperature reduced the surface tension and viscosity low enough for the kinetic energy to be sufficient to promote jetting. However, jetting is not the only characteristic that needs to be controlled: the drop speed is also important. If the drop speed is too slow, the ink volume delivered to the substrate could be too low, leading to incomplete coverage or an insufficient ink film thickness to meet the desired electrical property requirements. Furthermore, a slow drop speed often results in the misdirection of the ink droplets as they travel towards the substrate. Thus, to obtain good print quality, the cartridge temperature and drop speed must be properly adjusted. The drop speed is adjusted by altering the firing voltage. The drop volume is adjusted by altering the waveform. For this ink, the best jetting and print quality was accomplished at a drop speed of 4 m/s and cartridge temperature of 47°C.[10] Using this setup, a 1 cm by 0.5 cm pattern was printed at three different drop spacings (10 μm (2540 dpi), 20 μm (1270 dpi), and 30 μm (847 dpi)) to obtain ink films of different thicknesses. Figure 3(a) shows the applied waveform for the nano-copper ink where proper positive and negative voltage are generated to enable the ink eject through the nozzles, resulting in uniform drops without satellite drops, as shown in (b). The red mark on the

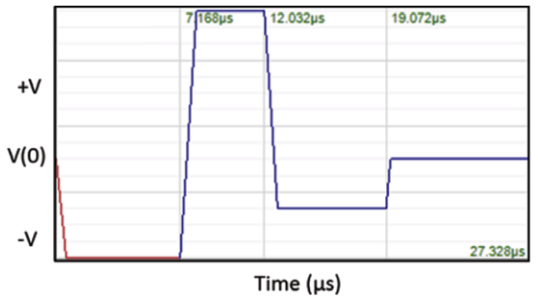

(a)

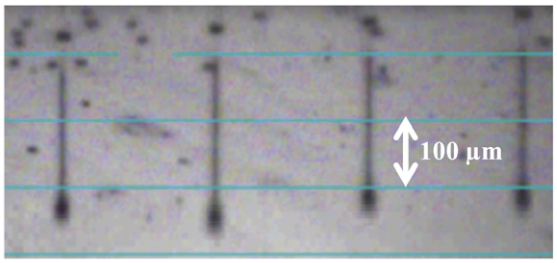

(b)

Figure 3. The waveform (a) used in the printer and ink ejection for nano-copper ink (b).

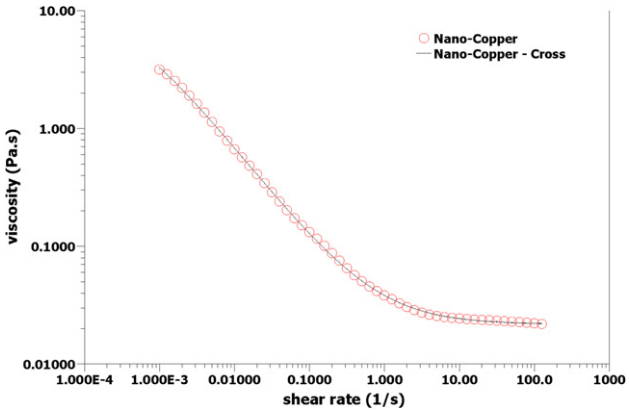

Figure 4. The result of rheological behavior for nano-copper ink.

Table I. The results of Cross model analysis.

Sample name	η_0 [Pa s]	η_∞ [Pa s]	K [s]	m	Standard error (%)
Nano-copper	11.8	0.0217	3224	0.8121	4.787

waveform means the state of the printer where it works. The total time for one cycle of drop ejection was 27.32 µs.

The shear-thinning properties of the ink are shown in Fig. 4. As shown, the rheological properties of the ink are well fitted by the Cross model[14] (Eq. (3)), which combines the low shear viscosity (η_0), the high shear viscosity (η_∞), and the shear-thinning part of the curve by a two-parameter power law relationship. From the Cross model, K, the characteristic time of the material, and m, the degree of shear thinning, are obtained. These values are provided in Table I.

$$\eta = \frac{\eta_0 - \eta_\infty}{[1 + (K\dot{\gamma})^m]} + \eta_\infty. \quad (3)$$

The standard error is well below 20, meaning that the fit is very good. The results from the Cross model fits are summarized in Table I.

The initial deposition of the ink onto the PET film did not result in good ink wetting or ink adhesion. On the other hand, the ink printed well on the glass. The differences in results can be explained by the differences in the surface energies. As shown in Table II, the surface energy of the glass, 63.7 dyne/cm, is much higher than that of the PET film, 43.8 dyne/cm.

Table II. Surface energy values of substrates; unit: dyne/cm.

Name	Surface tension	Surface energy	Dispersive	Polar
Nano-Cu	29.8 ± 1.2	—	—	—
PET	—	43.8	2.3	41.8
UV/ozone-treated PET (275 s)	—	62.7	46.2	16.5
Glass	—	63.7	47.4	16.4

To alleviate the problem, the surface energy of the PET was increased to 62.7 dyne/cm by application of a UV/ozone treatment. The change in surface energy of the film with the UV/ozone exposure time is shown in Figure 5. The surface energy of the film greatly increased after 100 s of exposure. Before treatment, the ink film was rough, and beaded ink drops are observed. After treatment, the ink film was smooth.

Application of the UV/ozone treatment for 270 s increased the surface energy from 43.8 to 62.7 dyne/cm. The treatment especially affected the dispersive energy component of the surface energy value (Table II). This is in agreement with Ton-That et al.,[15] who reported that the π bonding of phenyl groups in the PET is broken by absorbing UV energy, which leads to an increase in the number of ester groups at the surface. The greater the exposure time, the greater the number of ester groups through which the oxidization readily takes place, resulting in larger grains at the surface of the treated PET than at that of untreated PET. The grain size is proportional to the roughness. Therefore, exposure of the film to UV/ozone roughens the surface of the film, which for a hydrophilic substrate raises the surface energy in accordance with the Young–Laplace equation.[16,17] The increase in PET film surface energy improved the print quality of the nano-copper ink.

The experimental design followed for sintering the substrates is shown in Table III. The energy applied was altered by changing the voltage of the lamp and time of printed sample exposure. As shown, the total energy applied was varied from 5175 to 10 909 J. The optimized total electrical energies for the samples printed at 10, 20 and 30 µm drop spacings were 10 909, 5455, and 5175 J, respectively. Under these conditions, the lowest resistance obtained was 1.4 ± 0.2 Ω/□. Since sample No. 1 was printed with a

Table III. The experimental design followed for altering the amount of energy applied to the nano-copper printed PET film.

Sample No.	Drop spacing (μm)	Pulse width (μs)	Capacitance (μF)	Applied voltage (V)	Applied times (s)	Distance (inch)	Total electrical energy (J)	Resistance (Ω/□)
1	10	500	115	3080	10	1	10 909	1.4 ± 0.2
2	10	500	115	3080	5	1	5455	Not dried
3	10	500	115	3000	5	1	5175	Not dried
4	20	500	115	3080	10	1	10 909	>105 M*
5	20	500	115	3080	5	1	5454.6	6.18 ± 0.42
6	20	500	115	3000	5	1	5175	$47k \pm 6k$
7	30	500	115	3080	10	1	10 909	>105 M*
8	30	500	115	3080	5	1	5455	>105 M*
9	30	500	115	3000	5	1	5175	20.0 ± 0.3

* Greater than the measurable impedance of the instrument used.

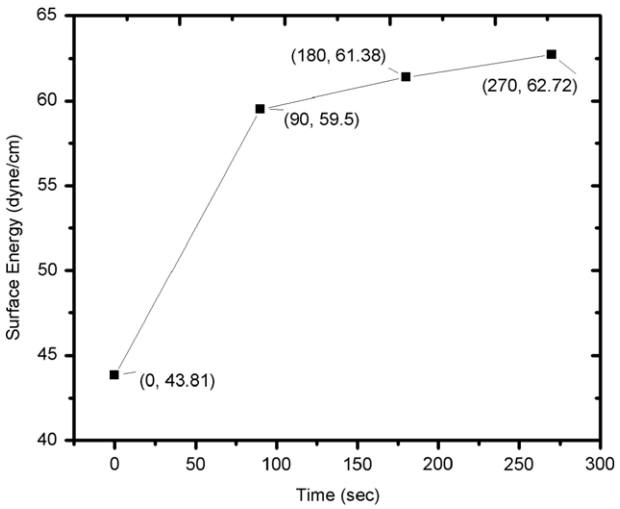

Figure 5. Influence of UV/ozone treatment on PET with time.

drop spacing of 10 μm, it had the highest ink film thickness (595 nm) prior to exposure to the xenon lamp. Therefore, this was the sample used to approximate the conditions needed for sintering the other samples (No. 5 and No. 9) of thinner ink film thicknesses (110 and 62 nm, respectively). Likewise, the sintering condition for sample No. 9, printed at a drop spacing of 30 μm, was used to estimate the energy required for sintering sample No. 6, printed with a drop spacing of 20 μm. The amount of energy applied for sample No. 1 and sample No. 5 caused damage to sample No. 7 and sample No. 8. The influence of IPL energy on the morphology of the inks can be seen from the SEM images shown in Figure 6. Since the energy intensity of the spiral lamp decreases as the sample is further away from the center of the lamp, the influence of lamp energy on particle sintering could be obtained.

There was a space of 2.54 cm between each position (a), (b), and (c), where (a) is the center of the lamp. From the SEM micrographs, it is clear that, as the energy applied increases, fewer individual nanoparticles are present as a result of particle sintering.

Figure 7 shows the x-ray diffraction (XRD) pattern for the copper ink before and after sintering the samples printed with different drop spacing. The sintered XRD pattern shows two characteristic peaks at 43.56° and 50.80°. The peaks verify the presence of the face-centered cubic (FCC) copper phase without any oxidization or other impurity phases being present after IPL sintering. The increase in Cu peaks with decrease in drop spacing indicates that the amount of coalescence of Cu increased.

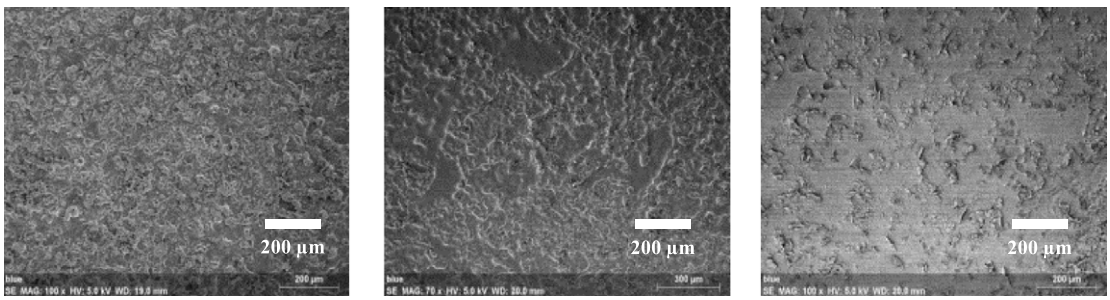

a). Applied energy: 5454 J — b). Applied energy: 4800 J — c). Applied energy: 3709 J

Resistance: 6.18 Ω/□ — Resistance: 7.2 Ω/□ — Resistance: >105 Ω/□

Figure 6. SEM micrographs of sintered samples (magnification 100 ×).

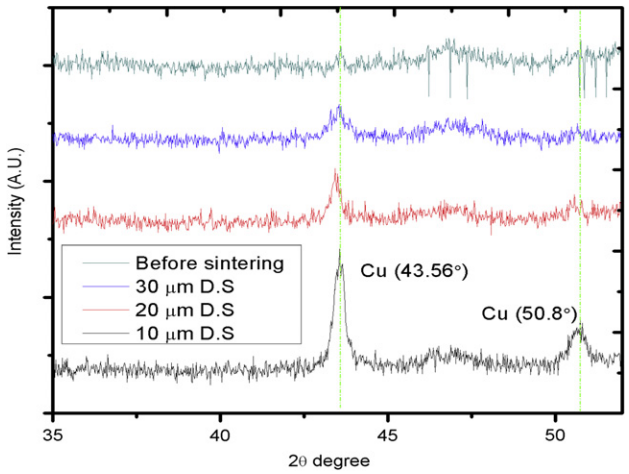

Figure 7. XRD patterns of nano-copper ink sintered using light intensity of 10 909 J on samples printed from 10 to 30 μm drop spacing interval.

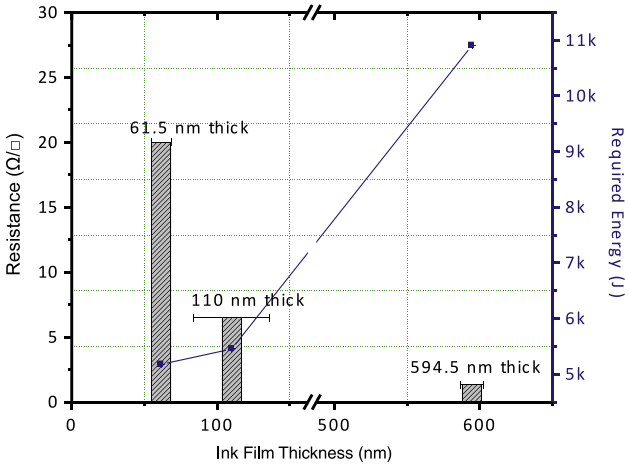

Figure 8. Relation between average ink film thickness and required energy for sintering nano-copper ink on PET.

Figure 8 shows the relationship between ink film thickness and sintering energy requirements. The relationship between sintering energy and resistance is also shown. The energy required for sintering is proportional to the ink film thickness, while the resistance is inversely related to the ink film thickness. The resistance decreased with increased ink film thickness, as a result of more nano-copper particle-to-particle contact in the printed ink film.

The surface topography of the printed samples before and after sintering is shown in Figure 9. Since the surface roughness of the base film (PET) is less than 10 nm (as reported by the manufacturer), the vacuum-oven-dried ink film is very smooth (Fig. 9a). After sintering, the roughness is shown to dramatically increase, Fig. 9(b), due to the movement and cohesion of the nano-Cu particles and burn off of carrier solvent within the ink and other ink components. The measured roughness of almost 410 nm for the 10 μm spacing is a significant percentage of the original film thickness of almost 600 nm. Similar roughness ratios to ink film thickness were seen for the wider drop spacings. The electrical performance of the rough film could likely be improved by calendering[18] after sintering.

In addition to determining the influence of ink film thickness on sintering energy requirements, the influences of the substrate thermal properties on sintering energy requirements were also determined by comparing the energy required to sinter the nano-copper ink on a transparent 614 μm thick glass and 127 μm thick PET. Since the glass had a similar surface energy to that of the UV/ozone-treated PET, it did not have to be treated before printing. Both substrates were printed at a drop spacing of 20 μm. Application of 5455 J (sample 5 in Table II) of energy was insufficient to sinter the particles on glass. Instead, significantly more energy (about 10 times more) was needed. This application of higher energy resulted in a resistance of 68.9 ± 9.5 Ω/□, but, unfortunately, the adhesion of the copper ink on the glass was poor. The reason for this finding can be explained as follows: suppose that an IPL with 1 J/cm^2 is irradiated onto a 10 μm thick nano-copper ink film printed over 127 μm thick PET film and 614 μm thick glass film. Assume further that all of the light energy is absorbed into both layers without scattering and reflection. Then, based on these assumptions, the increase in temperature for all the materials can be estimated by use of the lumped mass method as follows:[3]

$$\Delta T = \frac{E}{\rho C_p V} = \frac{E}{\rho C_p A t} = \frac{Energy\ Density}{\rho C p t} \qquad (4)$$

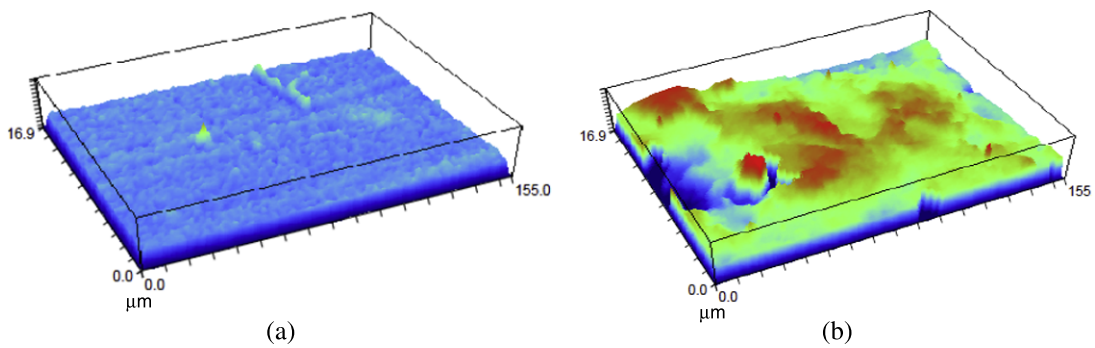

Figure 9. Surface morphology of unsintered ink film (a) and sintered film (b). All films were printed using at a drop spacing of 10 μm.

Table IV. Thermal properties of materials.[19,20]

Material	Thermal conductivity (W/mK)	Heat capacity (J/g/K)	Density (g/cm^3)	Melting temperature (°C)
Copper	170	0.386	8.71	1084
Polyethyleneterephthalate (PET)	0.14	1.3	1.39	255
Glass	0.01	0.768	2.38	No data

where ρ, C_p, A and t are the density, the heat capacity, area, and the ink film thickness, respectively.

Using the thermal properties of the materials provided in Table IV, sintering produces an increase in the copper, PET, and glass film temperatures to 297, 43.5, and 8.9°C, respectively. Since the PET and glass are both poor thermal conductors, as shown in Table IV, the copper plays an important role in the adhesion between the substrates by melting the substrate at the ink interface. For the glass, there was only an 8.9°C increase in temperature, which is about 5 times lower than that of the PET. This temperature difference explains the poor adhesion of the copper to glass in comparison to the PET.

CONCLUSION

In order to sinter the nano-copper ink printed onto a PET film under ambient conditions, an intensive pulsed light (IPL) treatment was applied. The effect of ink-jetting conditions and sintering, without preheating, was studied. The relationship between the ink film thickness and the energy required for sintering the amount of bridging present increased with the amount of energy applied. Overexposure of the samples to the xenon lamp resulted in damage to the printed samples and loss in electrical properties. The influence of the thermal conductivity properties of the substrate on sintering energy requirements for the nano-copper ink was also determined by use of the lumped mass method.

REFERENCES

[1] B. K. Park, D. J. Kim, S. H. Jeong, J. H. Moon, and J. S. Kim, "Direct Writing of copper conductive patterns by ink-jet printing," Thin Solid Films **515**, 7706–7711 (2007).

[2] T. Cuk, S. M. Troian, C. M. Hong, and S. Wagner, "Using convective flow splitting for the direct printing of fine copper lines," Appl. Phys. Lett. **77**, 2063 (2000).

[3] H. S. Kim, S. R. Dhage, and D. E. Shim, "Intense pulsed light sintering of copper nanoink for printed electronics," Appl. Phys. A **97**, 791–798 (2009).

[4] D. J. Kim and J. H. Moon, "Highly conductive ink jet printed films of nanosilver particles for printable electronics," Electrochem. Solid-State Lett. **8**, J30–J33 (2005).

[5] S. H. Ko, H. Pan, C. P. Grigoropoulos, C. K. Luscombe, M. J. Frechet, and D. Poulikakos, "Air stable high resolution organic transistors by selective laser sintering of inkjet printed metal nanoparticle," Appl. Phys. Lett. **90**, 141103 (2007).

[6] W. S. Han, J. M. Hong, H. S. Kim, and Y. W. Song, "Multi-pulsed white light sintering of printed Cu nanoinks," Nanotechnology **22**, 395705 (6pp) (2011).

[7] P. Reip, "Developments in nanoscale metal inks for Printed Electronics," *Plastic & Printed Electronics: Interconnects & Manufacturing Challenges*, Loughborough University, 19th 2012.

[8] A. B. Godfrey and A. Kong, "Fine particles," US Patent 20120003392 A1 (Jan 5 2012).

[9] D. K. Owens and R. C. Wendt, "Estimation of the surface free energy of polymers," J. Appl. Pol. Sci. **13**, 1741 (1969).

[10] S. Lim, P. D. Fleming, and M. Joyce, "A study of the jetting evolution of nano copper ink and nano silver ink with inkjet," JIST **57**, 020506 (2013).

[11] N. Reis, C. Ainsley, and B. Derby, "Ink-jet delivery of particle suspensions by piezoelectric droplet ejectors," J. Appl. Phys. **97**, (2005)094903-6.

[12] Xenon, Pulsed UV Lamps, http://xenoncorp.com/uv_spectrums.html, accessed 6/14/2013.

[13] V. Fakhfouri, G. Mermoud, J. Y. Kim, A. Martinoli, and J. Brugger, "Drop-On-demand inkjet printing of SU-8 polymer," Micro and Nanosystems **1**, 63–67 (2009).

[14] M. M. Cross, "Rheology of non-Newtonian fluids: A new flow equation for pseudoplastic systems," Colloid Sci. **20**, 417 (1965).

[15] C. Ton-That, D. O. H. Teare, P. A. Campbell, and R. H. Bradley, "Surface characterisation of ultraviolet-ozone treated PET using atomic force microscopy and X-ray photoelectron spectroscopy," Surf. Sci. **433**, 278 (1999).

[16] T. Young, Miscellaneous Works, G. Peacock, ed., Miscellaneous Works, J. Murray, London, 1, 418 (1855).

[17] P. S. de Laplace, Mechanique Celeste, "Mechanique Celeste," Supplement to Book 10, (1806).

[18] P. D. Fleming, M. K. Joyce, M. Rebros, D. Al-Said, E. Hrehorova, and M. Stoops, "Development of in-line printing press calendering station," *Proc. IS&T's NIP26: Int'l. Conf. on Digital Printing Technol. and Digital Fabrication 2010* (IS&T, Springfield, VA, 2010), p. 657.

[19] DuPont, "Displays, Products & Services" http://www2.dupont.com/Displays/en_US/products_services/films/PET_films.html, accessed 6/14/2013.

[20] D. L. Young, K. Alberi, C. Teplin, I. Martin, P. Stradins, M. Shub, C. Beall, E. Iwaniczko, H. Guthrey, M. J. Romero, T.-K. Chuang, E. Mozdy, and H. M. Branz, "Toward film-silicon solar cells on display glass," *IEEE PV Specialists Conference* 35; June 20, 2010.